Available online at www.sciencedirect.com
ScienceDirect
Journal of Power Sources 175 (2008) 502–509
JOURNAL OF POWER SOURCES
www.elsevier.com/locate/jpowsour

Mesoporous Cr_2O_3 as negative electrode in lithium batteries: TEM study of the texture effect on the polymeric layer formation

L. Dupont [a,*], S. Laruelle [a], S. Grugeon [a], C. Dickinson [b], W. Zhou [b], J.-M. Tarascon [a]

[a] *Laboratoire de Réactivité et de Chimie des Solides, UMR 6007, Université de Picardie Jules Verne, 33 rue Saint-Leu, 80039 Amiens Cedex, France*
[b] *School of Chemistry, University of St. Andrews, St. Andrews, Fife KY16 9ST, United Kingdom*

Received 13 July 2007; received in revised form 21 September 2007; accepted 23 September 2007
Available online 2 October 2007

Abstract

Mesoporous single crystal (PSC) oxides have been reported as presenting higher electrochemical performances than bulk materials in lithium ion batteries operating via intercalation processes. Here, we extend this study to the electrochemical behaviour of mesoporous Cr_2O_3 versus Li^+/Li^0. We confirm that the Cr_2O_3 reacts towards Li through a conversion reaction mechanism leading, upon discharge, to the formation of large metallic chromium nanoparticles (10 nm); the latter are embedded into a Li_2O matrix together with, in this specific case, a copious amount of polymeric materials coming from electrolyte degradation, surrounding the particles, and filling the pores. During the following charge, re-oxidation of the nanoparticles occurs with the formation of CrO_{1-x}, with the main difference, as opposed to bulk Cr_2O_3 electrodes, being the preservation of the polymeric layer at the end of the charge. We believe the material mesoporosity, via capillary effects, to be at the origin of such a difference. These electrolyte degradation products are shown to help in maintaining the material mesoporosity for a great number of cycles; and interestingly they are not detrimental to the cell performance in terms of capacity retention while presenting great advantages in terms of charge transfer by reducing diffusion lengths, namely for Li^+ ions. The positive attributes of mesoporous material-based electrodes noticed for insertion reactions can then be extended to conversion reaction electrodes as long as we can master their synthesis while controlling their mesoporosity through either soft or hard templating techniques.

Keywords: Mesoporous; Chromium oxide; Conversion; Lithium battery; Electron microscopy; Electrochemistry

1. Introduction

Commercial Li-ion batteries operate by an electrochemical process that involves intercalation reactions both at the positive and negative electrodes. Presently, the materials used as the positive electrodes such as $LiCoO_2$, $LiMn_2O_4$ or even $LiFePO_4$ cannot react with more than one lithium per 3d-metal. They are combined with carbonaceous negative electrode materials that can reversibly react to Li (e.g. LiC_6) to give practical capacities of about 372 mAh g^{-1} as compared, for instance, to 3600 mAh g^{-1} for Li metal. Aware of such a wide improvement window, intense research has been carried out worldwide to develop alternative negative electrode materials having greater performances than graphite. Such research is mandatory if the Li-ion systems are ever to attain the performances required by new automotive applications. Within this context, the research was parted between revisiting previously disregarded materials and searching for new directions [1–5]. The most promising candidates have long been the metal elements capable of forming alloys with Li, such as Si (4200 mAh g^{-1}) [4] or Sn (1200 mAh g^{-1}) [5]. However, owing to the poor efficiency of the Li alloying/de-alloying process leading to poor long-term stability, research teams have progressively shifted their interest to either amorphous tin composite oxides (ATCO) [6], composite negative alloy electrodes such as $Sn_2Fe/SnFe_3C$ [7] or intermetallic such as Cu_6Sn_5 [8] and finally to composite negative electrodes containing metallic element nanoparticles [9].

Back to 2000, searching for another path to improve the negative electrode capacity, our group had investigated the reactivity of metal oxides having a compact crystal structure (e.g. CoO) towards Li; they spotted a new Li reactivity mechanism called

* Corresponding author. Tel.: +33 322827585; fax: +33 322827590.
E-mail address: loic.dupont@sc.u-picardie.fr (L. Dupont).

0378-7753/$ – see front matter © 2007 Elsevier B.V. All rights reserved.
doi:10.1016/j.jpowsour.2007.09.084

"conversion reaction" enlisting a two to four e^- reversible charge transfer per 3d-metal [10–12], as compared to solely one for insertion reaction, leading then to outstanding capacity gains. Potential wise, the most interesting oxide to be used as negative electrode material for Li-ion cell would be Cr_2O_3 [9] as it shows the lowest redox potential versus Li. Indeed, during the first discharge, chromium oxide particles react with lithium at 0.3 V to form an agglomerate of nanometric metallic chromium particles embedded in the Li_2O matrix. During the following charge taking place near 1.2 V, the nanoparticles are partially re-oxidized into chromium monoxide. However, the charge/discharge transfer limitations associated with the poor electronic properties of binary oxides and reflected by the large polarisation between charge and discharge curves (e.g. 0.9 V) result in a poor energy efficiency, which compromises the implementation of these compounds in the next generation of lithium-ion battery. To address this problem, besides the chemical approach consisting in studying the effect of nature of the anion on the polarisation for various families of binary MX compounds (X = S, N, P, F,), our group engineered a new electrode design. It consists in growing, through appropriate thermal treatments under different atmospheres [12,13], a chromium-rich oxide layer on top of a stainless steel current collector. Owing to the high quality current collector-electroactive Cr_2O_3 the so-obtained nanotextured electrodes have large capacities and outstanding cycling performances versus Li for more than 800 cycles.

A strong enhancement of cycleability has also been reported for many other materials, whether reacting with Li through an insertion or conversion process, as soon as mesoporous structures were involved [14–20]. Such structures induce a large surface area and a thin pore wall reducing the lithium ion diffusion path. The most impressive result on mesoporous MnO_2 was reported by Jiao and Bruce [15] and Luo et al. [14]. Bulk state β-MnO_2 is electrochemically inactive while mesoporous electrodes can reversibly react with 0.92 lithium, and preserve the porosity during cycling. Moreover, Bruce's group recently reported the successful use of mesoporous Co_3O_4 conversion reaction electrodes as negative electrodes for rechargeable lithium batteries [20].

Based on our previous work on the Cr_2O_3 electrode and seeking to support the fundamental viability of the mesoporous single crystal concept for enhanced electrode performances, we embarked in the study of the electrochemical reactivity of mesoporous Cr_2O_3 versus Li. The results of such a full electrochemical, structural, textural and analytical study are reported herein; the highlight is that having a mesoporous electrochemical active material is not always a positive attribute for a performance standpoint.

2. Experimental

2.1. Electrochemical tests

Electrochemical tests versus lithium were performed using coin cells (standard 2035-size) that were assembled in an argon filled dry-box. The studied sample was separated from a lithium disk used as the negative electrode by a borosilicate micro-fibre (Millipore) film impregnated with 0.5 ml of a $LiPF_6$ (1 M) in EC-DMC (1-1) solution. All the experiments were carried out using a VMP system (Biologic S.A., Claix, France) that can be operated in both potentiodynamic and galvanostatic modes (one lithium in 8 h, corresponding to a *C*/40 rate) at 55 °C in the 0.02–3 V potential window. All reported potential values are given versus Li/Li^+.

2.2. Analytical high resolution transmission electron microscopy

Transmission electron microscopy (TEM) was carried out using a FEI TECNAI F20 ST microscope, equipped with both energy dispersive X-ray spectroscopy (EDS) analysis capabilities and a home designed sample holder for moisture sensitive samples. The studied samples, coming from cycled coin cells opened in an argon-filled glove box, were recovered and washed with acetonitrile prior to being placed onto a copper grid mounted on our TEM sample holder. Recorded selected area electron diffraction (SAED) patterns were converted in equivalent XRD pattern (Cu Kα radiation) using the process

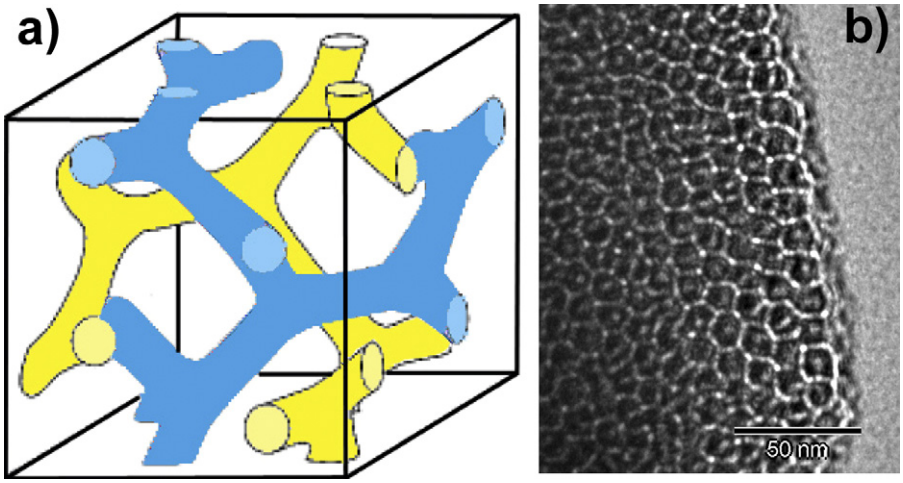

Fig. 1. (a) Structure model for cubic Ia3d mesophase and (b) TEM image of the KIT-6 along [1 1 1].

diffraction software [21] in order to determine the implied phases.

2.3. Mesoporous Cr_2O_3 synthesis

Mesoporous single crystal chromium oxide was obtained according to the synthesis method proposed by Dickinson et al. [22]. Chromium(III) nitrate nonahydrate ($Cr(NO_3)_3{\cdot}9H_2O$) was dissolved in 6.5 g ethanol and stirred for 2 h with 0.15 g of KIT-6 silica, which was freshly prepared according to literature [23]. KIT-6 has a cubic symmetry, space group *Ia*-3*d*, and contains a 3D cubic arrangement of bi-continuous channels organized in two enantiomeric interwoven systems (Fig. 1a) giving birth to an hexagonal symmetry along the [1 1 1] direction as observed on the corresponding bright field image (Fig. 1b). The ethanol evaporated at approximately 40 °C. During the ethanol evaporation process, the metal nitrates were drawn into the zeolite mesopores by capillary action. The chromium nitrate was then thermally decomposed (temperature heating rate of 2 °C min^{-1} from room temperature to 550 °C and maintained at that temperature for 5 h) to lead to the growth of chromium oxide crystals inside the KIT-6 channels. The KIT-6 silica framework was then removed by dissolving it in an aqueous solution 10 wt% HF. The clear solution was centrifuged and let to decant, after which the remaining powder was washed twice with water.

3. Results and discussion

3.1. Electrochemical study

The potential/composition curve obtained for mesoporous Cr_2O_3/Li cell is compared (Fig. 2a) with that of a previously reported bulk Cr_2O_3/Li cell cycled under similar conditions [12]. Their first discharge proceeds via a conversion reaction mechanism leading to the formation of metallic chromium particles embedded into a Li_2O matrix with therefore a better reactivity (e.g. one more Li^+) for the mesoporous as compared to the bulk

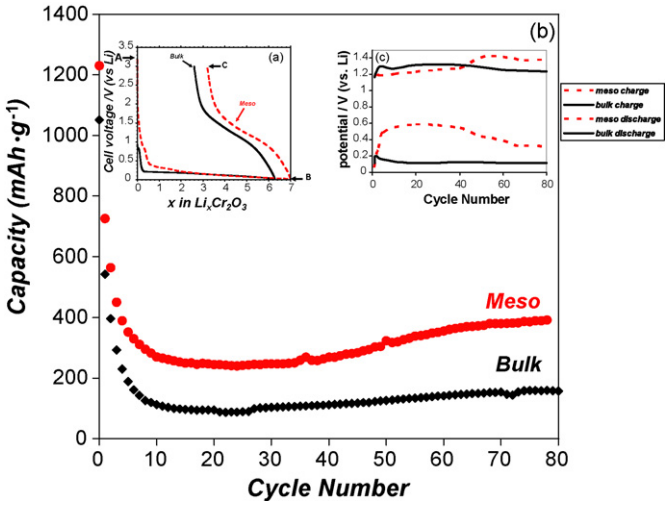

Fig. 2. (a) First charge–discharge curves, (b) capacity retention and (c) polarisation between reduction and oxidation potentials as function of cycle numbers for bulk and mesoporous Cr_2O_3 cycled in the same conditions.

Cr_2O_3 electrode. Upon subsequent charge, the voltage smoothly and continuously increases from 0.02 to 3 V with an overall release of 3.8 Li in agreement with the re-oxidation process $2Cr + 2Li_2O \rightarrow 2CrO + 4Li^+ + 4e^-$. Therefore, the irreversible capacity of the first cycle is larger for the mesoporous Cr_2O_3 electrode. For both electrodes, we note during the first 15 cycles a strong decrease in the cell capacity reaching 20 and 10% of the initial cell capacity for mesoporous and bulk oxides, respectively. Then the cells were found to stabilize with even a weak recovery of the capacity upon cycling as previously reported for conversion reaction electrodes. Whatever the number of cycle, the capacity of the mesoporous phase is higher than the one of the bulk (Fig. 2b). Moreover, by reporting the potential of the charge and discharge plateaus (as deduced by the values of peaks in the derivative d*x*/d*V* curves) versus the number of cycles (Fig. 2c), we can highlight a strong decrease in polarisation for the mesoporous cell compared to the bulk, at least for the first 40 cycles. Afterwards, the polarisation becomes similar again. Although we do not have a clear explanation for such behaviour yet, we can ascertain that it is real since each reported cell data was duplicated.

In light of such study, many questions arise such as why is not the mesoporous texture of Cr_2O_3 particles that beneficial to its overall electrochemical performances (enhanced initial irreversibility, rapid capacity decay during the first 15 cycles, and changing polarisation upon cycling) while the opposite was clearly observed on cobalt oxide [20]? In an attempt to throw some light on the origin of this difference, analytical and TEM studies were conducted, as presented hereunder, for samples denoted A, B and C on the first cycle trace (Fig. 2a), and corresponding to a fresh, fully discharged and fully recharged mesoporous Cr_2O_3, respectively. The D sample was recovered after 80 cycles.

3.2. Analytical and TEM studies

3.2.1. Starting material

Although the starting material was intensely characterized elsewhere [22], we should recall for sake of comparison its main characteristics in terms of crystallinity, shape and size. The mesoporous Cr_2O_3 particles grown according to the template-assisted synthesis process crystallized according to the Eskolaite structure with the following cell parameters: $a = 4.9538(6)$ Å, $c = 13.585(2)$ Å, S.G. = *R*-3*c* (Fig. 3a). TEM images (Fig. 3b) indicate that the original KIT-6 mesoporous system was replicated, as shown on the [1 0 0] (particle on the left showing square symmetry tunnels) and [1 1 1] (particle on the right showing hexagonal channels). This structural character indicates that only one of the bi-continuous (two different networks) pores in KIT-6 has been replicated by Cr_2O_3. This differs from the KIT-6 templated porous crystals of Co_3O_4, in which both pores are replicated [22,24]. Consequently, in comparison with porous Co_3O_4 made from the same template, the specific surface area of Cr_2O_3 slightly reduces. High resolution TEM (HRTEM) images (Fig. 3c) show that each particle is a porous single crystal (PSC) since continuous lattice fringes are nicely observed on the whole particle with walls and pores measuring both 10 nm. This visual

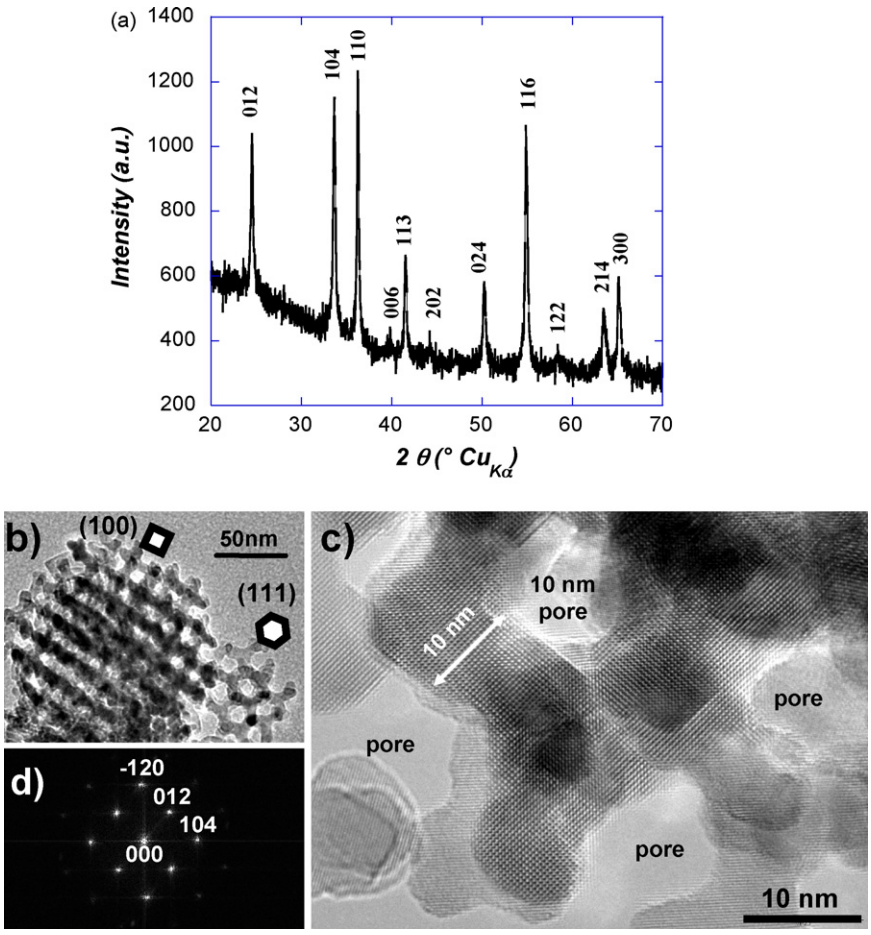

Fig. 3. (a) X-ray diffraction pattern as well as (b) bright field, (c) high resolution transmission electron microscopy images and (d) corresponding selected area electron diffraction pattern of the mesoporous starting material.

impression is undeniably confirmed by the corresponding [4, 2, −1]* zone axis SAED pattern (Fig. 3d) showing well-defined dots proving the existence of a single crystal.

3.2.2. *Discharged sample*

Particles obtained after reduction down to 0 V through a conversion reaction process were usually shrouded in a thick polymeric layer. This layer, well known to be responsible for extra-capacity in conversion reactions, covers not only the particles but also fills up the pores (Fig. 4a). This effect is especially visible if we compare the same region before (Fig. 4a) and after long beam exposure (Fig. 4c). In order to strengthen this idea, a TEM image of discharged bulk material is given in Fig. 5a. For such an electrode, at the end of the first cycle, the quantity of electrolyte decomposition products (EDP) is moderate since only a thin localized polymeric layer is observed. Thus, the specific texture of our porous material, via its large surface area and the possibility for the electrolyte to enter the 10 nm pores, could explain the formation of this large amount of EDP and consequently the increase in extra-capacity for the PSC Cr_2O_3 compared to other electrochemically tested Cr_2O_3 sample (Fig. 2a). The quantity of EDP is so large that lithium carbonate, known as one of the constituents of the EDP layer (namely the inorganic part), was undeniably observed, for the first time to our knowledge, on a SAED pattern (Fig. 4b). This lithium carbonate is usually detected by Infrared spectroscopy analysis; needless to say that IR measurements (not shown here) performed on this sample have confirmed a copious amount of Li_2CO_3.

The use of a condensed TEM electron beam, owing to the local heating, provokes the disappearance of the organic species of EDP. Such electrolyte blasting is so huge that it sweeps along the departure of most of the lithium carbonate, leaving behind (Fig. 4c) metallic chromium nanoparticles embedded into a Li_2O matrix (Fig. 4d), in agreement with the conversion mechanism. Note that the first lithia reflections are very weak while the metallic chromium ones are strong and almost punctual (the angle of the arc is very small) implying that the metallic chromium particles should not be as small and randomly oriented as usually observed for other discharged chromium oxides. HRTEM images (Fig. 6a and b) combined with FFT calculation (Fig. 6c) reinforce this assertion since large oriented chromium particles are observed. Indeed, pores are now surrounded by large metallic (more than 10 nm) and well-crystallized particles (Fig. 6b; squares) themselves surrounded by an amorphous area assigned to lithia. Although separated, the chromium particles present the same orientation (consequently the same FFT shown in Fig. 6c). Thus, the mesoporosity seems to induce a decrease in the constraints during the electrochemical process and minimize the

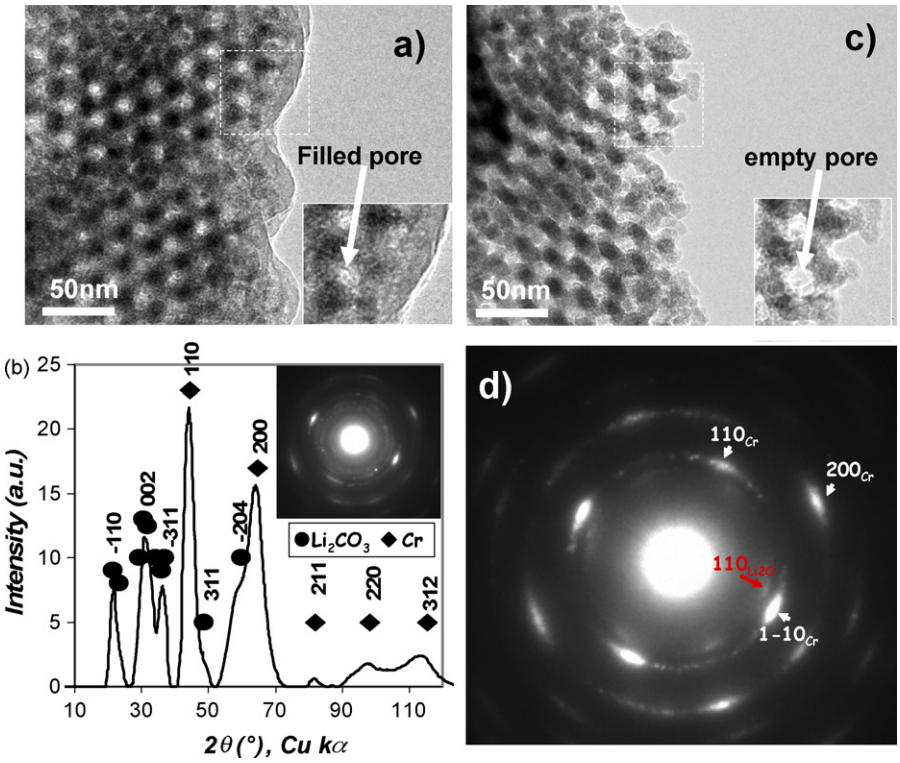

Fig. 4. TEM study of the discharged material (0.005 V). (a) Bright field image showing the filling of the pores by electrolyte degradation products with an enlarged view in inset. (b) SAED pattern showing, for the first time by this technique, the presence of lithium carbonate as part of the degradation products (strong and all reflections are reported for Li_2CO_3 and Cr, respectively). (c) Bright field image obtained after polymer vanishing using the electron beam (enlarged view in inset) and revealing (d) by SAED, the nature of the phases forming the particles.

corresponding grinding leading to metallic particles three times larger (10 nm versus 3 nm) than usual (such as nanoparticles obtained on discharged bulk particle in Fig. 5a). The pores, through the free space that they provided, seem to act as a volume buffer capable of accepting the theoretical 100% volume expansion associated to conversion reactions as deduced from simple cell volume calculations (from 48.08 $Å^3$ per Cr_2O_3 to 97.47 $Å^3$ per $2Cr + 3Li_2O$). Indeed, we assume that the created Li_2O moves toward the centre of the pore covering the particles thus minimizing the strains inside the material. Instead of having agglomerates formed by an intimate mixture of Li_2O and randomly distributed metallic nanoparticles, as usually observed during the reduced state of the conversion mechanism, one believes that the mesoporous texture, which is preserved during the process, favours the formation of larger chromium particles concomitantly with a blending of lithia and polymer overrunning the free spaces. This process is summarized in Fig. 6d.

3.2.3. Recharged sample

TEM images were recorded on both bulk and mesoporous Cr_2O_3 recovered from fully charged (e.g. 3 V) Cr_2O_3/cells. Strikingly, a copious part of EPD obstructing the pores is still observed (Fig. 7a) for the mesoporous sample as compared to the bulk one, which is nearly free of EPD (Fig. 5b) in agreement with previous findings. Moreover, we indirectly experienced that the nature of the polymer remaining in the charged state is somewhat different from the one observed during discharge since a long electron beam exposure does not lead to its vanishing. Besides,

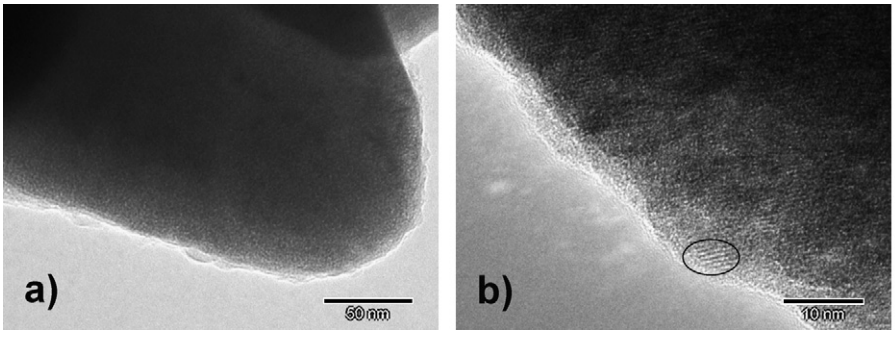

Fig. 5. TEM images realized on (a) discharged and (b) recharged bulk chromium oxide showing that polymeric layer is barely observed in discharge and absent in charge as well as the size of so-obtained nanoparticles (3 nm, as delimited by dark circle).

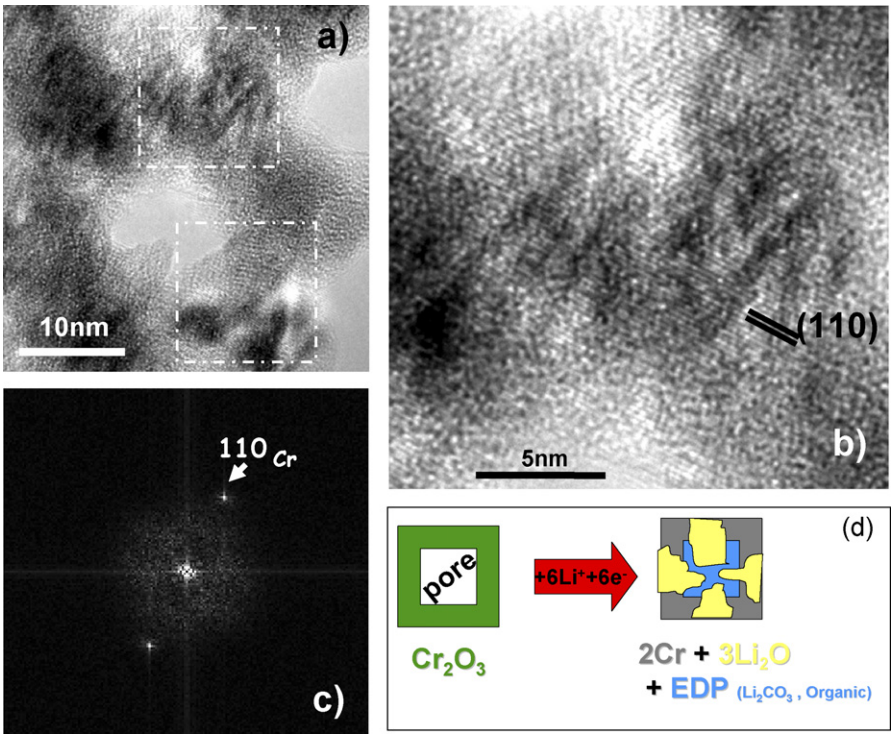

Fig. 6. HRTEM observation of the discharged material showing (a) and (b) large crystallized nanoparticles surrounding the pores and (c) oriented along the same direction. (d) Sketch of the particle obtained at the end of the reduction.

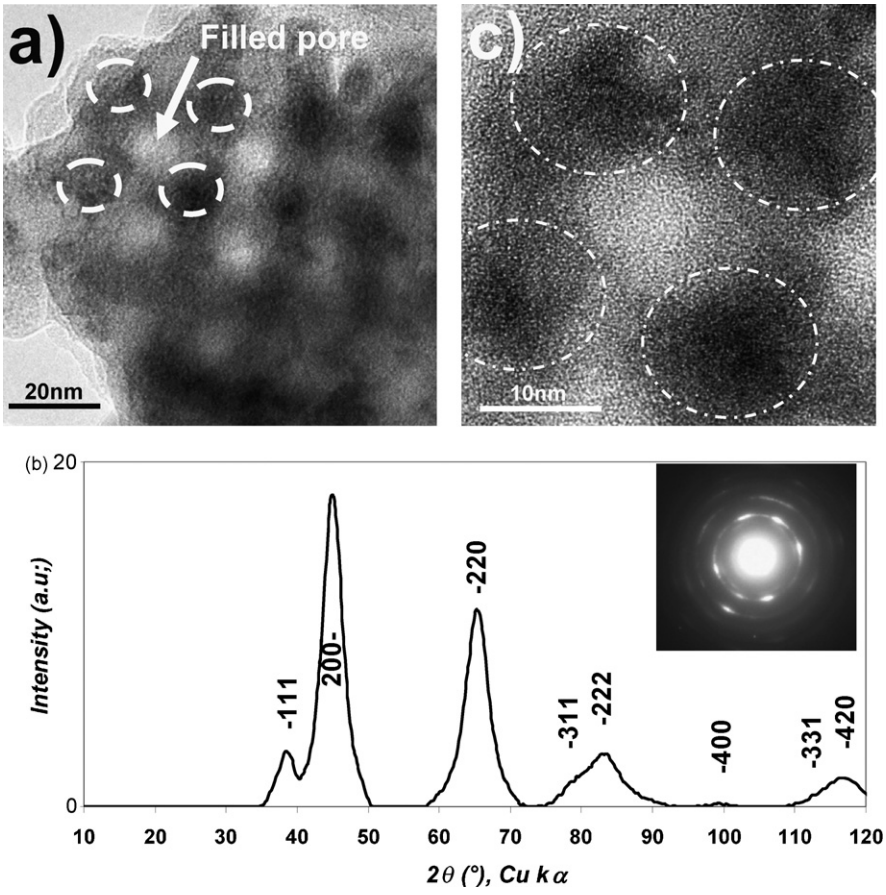

Fig. 7. TEM study of the recharged sample (up to 3.5 V) showing that (a) electrolyte degradation products are still sticking to the mesoporous particle made of (b) chromium monoxide (according to the SAED pattern forming (c) 10 nm nanoparticles surrounded by dashed white circles on the images.

well-crystallized nanoparticles of about 10 nm could nicely be observed (dashed white circles) on the HRTEM images, at the edges of the filled pores (Fig. 7c). Based on the corresponding SAED pattern (Fig. 7b) these crystallized nanoparticles could be indexed with $CrO_{0.87}$ cell parameters (according to the only CrO_{1-x} phase reported in the JCPDS files). This did not come as a surprise, as the formation of chromium monoxide rather than Cr_2O_3 during the recharge of a Li/Cr_2O_3 first discharged to 0 V is well known [12,13]; this explains the 33% irreversible capacity between charge and discharge during the first cycle.

At this juncture, we should stress that is the first time that such an amount of "electrolyte decomposition products" is created and/or preserved in charge. Among the most likely reasons is the mesoporous texture of the material; although previous studies on mesoporous transition metal oxide [14–20] and especially Co_3O_4 as negative electrode [20] did not reveal this phenomenon. The reason is probably nested in the redox potential of the Cr^{2+}/Cr^0 couple that is lower (0.4–0.5 V) than that of Co^{2+}/Co^0 (0.8–0.9 V) and hence favours larger amounts of EPD for Cr_2O_3 as compared to Co_3O_4 electrodes as observed experimentally and this regardless of the nature (bulk versus mesoporous) of the electrode material. Upon oxidation we have reported that the EPD vanishing mechanism involving both electrochemical/chemical reactions release soluble species. It is then conceivable that the "redissolution" of the EPD upon charging is considerably slowed down by the ratio EPD/electrolyte within the pore as compared to the surface of the bulk material. Interestingly, and confirming previous findings, such a large amount of electrolyte decomposition is not detrimental to the cell performance in terms of capacity retention (Fig. 2b). The only advantage of keeping a large amount of EDP during cycling is nested in the fact that this "glue" adds flexibility to the "composite material", and avoids the collapse and disintegration of the mesoporous texture, as would elastomer or filler. Simple theoretical cell volume calculations based on the oxidation reaction that should occur during the conversion reaction: $2Cr + 3Li_2O \Rightarrow 2CrO + Li_2O + 2Li^+ + 2e^-$ lead to a 40% volume shrinking. This boils down to a variation of solely 10% in the Cr/CrO particles radii assuming both a spherical model and a volume expansion/contraction solely nested in the breathing of the Cr/CrO particles. Usually, these volume expansions and contractions contribute to the electrochemical grinding, but in this specific case, they seem to be minimized by flexibility brought by the EDP in the pores. Therefore, a drawback associated to the large amount of EDP, clearly evidenced in Fig. 2, is the larger irreversible capacity for the mesoporous as compared to the bulk owing to the uptake of an extra Li on discharge that is not released on the following charge.

An evident advantage of mesoporous chromium oxide lies in (1) the grain size shortening, which enables a better fuelling of the electrons into the electrode although CrO is a poor electronic conductor [9] and (2) the specific material morphology that decreases the diffusion path for ions and enhances the access of cation in the electrolyte. Both effects are additives leading to an electrode based on mesoporous Cr_2O_3, and which shows a sustained capacity (Fig. 2) twice as large as that of the bulk. Such better electronic/ionic wiring of the electrode also accounts for the decrease in polarisation observed for the mesoporous electrode as compared to the bulk one, namely over the first 40 cycles (Fig. 2c). However, there still remains to understand why the polarisation increases after a long cycle up to the values of bulk materials. To answer this point, a TEM study of an electrode recovered after 80 cycles was performed.

3.2.4. *Long-term cycled material (80 cycles)*

In order to test the mechanical properties and sense the quantity of polymer filling the pores, we observed by TEM a sample recovered from a cell that was cycled 80 times and stopped in its charge state. Because of the particles being soaked (Fig. 8a) by a huge quantity of polymeric film resulting from cumulated amounts of electrolyte degradation upon cycling the mesoporosity of the cycled material cannot be easily detected. Nevertheless, we could still distinguish (Fig. 8b) the stamp of the KIT-6, with namely the square pores, surrounding spherical chromium oxide particles (or agglomerates) implying the preservation of the mesoporous architecture upon cycling. This is in contrast with TEM reports on mesoporous Co_3O_4 showing the initial preservation of its mesoporous texture during the first few cycles but its progressive deterioration upon subsequent cycling to the expense of a nano-composite structure somewhat similar to that observed for micron-sized particles. Such a change in structure was put forward by numerous authors to explain the decrease in capacity versus the cycle number observed for mesoporous. Our findings valid this previously established capacity retention–structural integrity correlation as our samples show

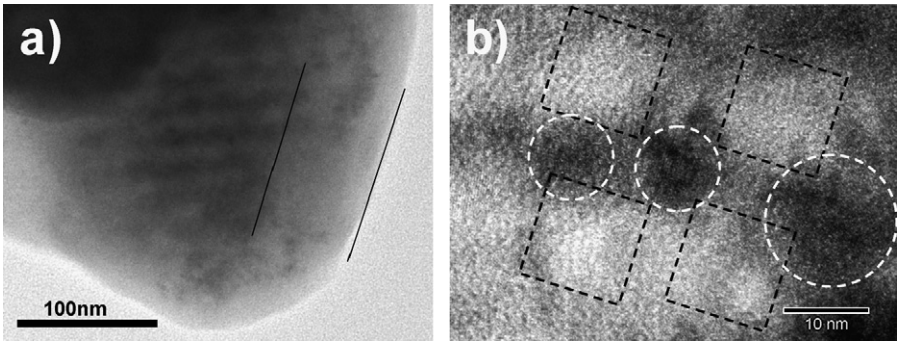

Fig. 8. TEM observation of the long-term cycled sample showing (a) the huge quantity of polymer surrounding the mesoporous particle and making (b) the pores and chromium nanoparticles hardly discernable. Black dashed squares and white dashed circles are used as guideline for pores and nanoparticles, respectively.

together sustained capacity retention and mesoporous structuring upon cycling.

Going back to the EDP layer surrounding the mesoporous crystal, its thickness reaches now several hundreds of nanometres. Therefore, the diffusion path for the ions coming from the outer becomes increasingly longer with increasing the cycle number, consequently, the polarisation increases up to the values of a classical bulk material. Nevertheless, this increase in polarisation does not affect the capacity retention. Quite the reverse, the capacity seems to increase (Fig. 1b) as previously observed with other oxides [25]. We are now investigating this point. There are several reasons to account for such a phenomenon. Indeed, we know that the chromium monoxide phase, obtained on the oxidized state, has oxygen defects. One hypothesis to explain the strange behaviour of polarisation and/or capacity retention versus the cycle number is linked to the variation of the number of anionic defects (CrO_{1-x}). Such evolution of the defects number will affect both the conductivity and reactivity of the oxide. Only EELS experiment, actually in progress, will allow checking such possible modification of nanoparticles oxides anionic defects versus cycle numbers. The greatest difficulty will be to record a reference spectrum for chromium monoxide, since the latter is very difficult to obtain in bulk state. Nevertheless, this spectrum could also be simulated and at least, the displacement (or not) in energy of the chromium edge will give some clue as to the possible evolution of the nature of the monoxide in charge.

4. Conclusions

The electrochemical reaction of lithium with mesoporous Cr_2O_3 has been investigated and compared to a bulk material (same oxide) as well as to another mesoporous oxide (Co_3O_4) that was previously studied [20]. The PSC chromium oxide reacts versus lithium according to conversion reaction as observed for all transition metal oxides [9] with therefore a greater capacity and better sustained reversibility than their bulk counterparts. Among the main reasons for such improvements is a better electronic/ionic wiring of the electrode owing to the specific electrode morphology that is also favourable to the formation of a polymer acting as a buffer layer with respect to the electrode volume changes. Unfortunately, such a polymer electrolyte formation that does occur via electrolyte degradation catalyzed by the electrode surface area can be counter productive with respect to the electrode performance if not totally mastered. In light of this study and with the goal of developing such a mesoporous low voltage material as negative electrode, we need to have the composition of both the material and the tailor-made electrolyte. The selected electrolyte should give a quantity of EDP sufficient to fill the pore and maintain the mesoporosity; but it should not give a thick surrounding polymer layer limiting electron and lithium access. On the other hand, the working potential of the electrode could be tuned, for instance, by playing with a transition metal substitution in the oxide. Iron is the perfect candidate since iron oxide also presents a low potential (slightly higher than the chromium one), a solid solution with chromium exists: $Cr_{2-x}Fe_xO_3$ ($0<x<2$), and finally a competition in anionic and cationic defects will occur during charge since iron monoxide is known as $Fe_{1-x}O$.

Acknowledgments

WZ thanks St. Andrews University for an EaSTCHEM studentship for CD.

LD thanks Alistore Network for the financial support, A. Débart and P.G. Bruce for many useful discussions.

References

[1] B. Scrosati, Nature 373 (1995) 557–558.
[2] J.-M. Tarascon, M. Armand, Nature 414 (2001) 359–367.
[3] W. Waklhara, O. Yamamoto (Eds.), Advances in Lithium-ion Batteries, Kodansha–Wiley–VCH, Wenheim, 1998.
[4] R.A. Huggins, J. Power Sources 13 (1999) 81.
[5] J.O. Besenhard, J. Yang, M. Winter, J. Power Sources 68 (1997) 87.
[6] Y. Idota, T. Kubota, A. Matsufuji, Y. Maekawa, T. Miyasaka, Science 276 (1997) 1395.
[7] O. Mao, J.R. Dahn, J. Electrochem. Soc. 146 (1999) 423.
[8] K.D. Kepler, J.T. Vaughey, M.M. Thackeray, Solid State Lett. 7 (1999) 307.
[9] S. Grugeon, S. Laruelle, L. Dupont, F. Chevallier, P.L. Taberna, P. Simon, L. Gireaud, S. Lascaud, E. Vidal, B. Yrieix, J.-M. Tarascon, Chem. Mater. 17 (20) (2005) 5041–5047.
[10] P. Poizot, S. Laruelle, S. Grugeon, L. Dupont, J.-M. Tarascon, Nature 407 (2000) 496.
[11] S. Grugeon, S. Laruelle, L. Dupont, J.-M. Tarascon, Solid State Sci. 5 (2003) 895.
[12] A. Débart, L. Dupont, P. Poizot, J.-B. Leriche, J.-M. Tarascon, J. Electrochem. Soc. 148 (2001) A1266.
[13] L. Dupont, S. Grugeon, S. Laruelle, J.-M. Tarascon, J. Power Sources 164 (2) (2007) 839–848.
[14] J.-Y. Luo, J.-J. Zhang, Y.-Y. Xia, Chem. Mater. 18 (23) (2006) 5618.
[15] F. Jiao, P.G. Bruce, Adv. Mater. 19 (2007) 657;
A. Débart, G. Armstrong, J. Bao, F. Jiao, M. Holzapfel, T. Ogasawara, P. Novak, P.G. Bruce, Meeting abstracts, electrochemical society 602 (2006) 367.
[16] F. Jiao, A. Harrison, P.G. Bruce, Angew. Chem. Int. Ed. 19 (2007) 657–660.
[17] P.G. Bruce, Solid State Sci. 7 (2005) 1456.
[18] F. Jiao, A. Harrison, J.C. Jumas, A.V. Chadwick, W. Kockelmann, P.G. Bruce, J. Am. Chem. Soc. 128 (2006) 5468.
[19] F. Jiao, K.M. Shaju, P.G. Bruce, Angew. Chem. Int. Ed. 44 (2005) 6050.
[20] K.M. Shaju, F. Jiao, A. Débart, P.G. Bruce, Phys. Chem. Chem. Phys. 9 (15) (2007) 1837–1842;
A. Débart, F. Jiao, P.G. Bruce, Abstract of the 208th ECS Meeting, Los Angeles, 2006.
[21] J.L. Labar, in: L. Franck, F. Ciampor (Eds.), Proceedings of EUREM 12, Brno, 2000, p. 1379.
[22] C. Dickinson, W. Zhou, R.P. Hodgkins, Y. Shi, D. Zhao, H. He, Chem. Mater. 18 (2006) 3088.
[23] F. Kleitz, S.H. Choi, R. Ryoo, J. Chem. Soc., Chem. Commun. 17 (2003) 2136.
[24] K. Jiao, B. Zhang, B. Yue, Y. Ren, S. Liu, S. Yan, C. Dickinson, W.Z. Zhou, H.Y. He, Chem. Commun. 45 (2005) 5618–5620.
[25] S. Grugeon, S. Laruelle, L. Dupont, J.-M. Tarascon, Solid State Sci. 5 (2003) 895–904.